

A tradeoff between protein stability and conformational mobility in homotrimeric dUTPases

Enikő Takács, Vince K. Grolmusz, Beáta G. Vértessy*

Institute of Enzymology, Hungarian Academy of Sciences, POB 7, H-1518, Budapest, Hungary

Received 3 February 2004; revised 3 April 2004; accepted 5 April 2004

First published online

Edited by Peter Brzezinski

Abstract Oligomerization directs active site formation in homotrimeric 2'-deoxyuridine triphosphate pyrophosphatases (dUTPases). Stability of the homotrimer is a central determinant in enzyme function. The present comparative studies of bacterial and fruitfly dUTPases with homologous 3D structures by differential scanning microcalorimetry; fluorescence, circular dichroism and infrared spectroscopies, demonstrate that unfolding is a two-state highly cooperative transition in both dUTPases excluding a significantly populated intermediate state of dissociated and folded monomers. The eukaryotic protein is much less resistant against either thermal or guanidine hydrochloride-induced denaturation. Results suggest that hydrophobic packing of the inner threefold channel of the dUTPase homotrimer greatly contributes to stability.
© 2004 Federation of European Biochemical Societies. Published by Elsevier B.V. All rights reserved.

Keywords: Stability; Oligomerization; Two-state unfolding; dUTPase; Microcalorimetry; Subunit interaction

1. Introduction

The 2'-deoxyuridine triphosphate pyrophosphatase (dUTPase) activity is indispensable to efficiently reduce cellular dUTP/dTTP ratios [1]. Elevated dUTP levels in lack of dUTPase result in erroneous incorporation of uracil into DNA. Uracil-substituted DNA induces hyperactivity of base-excision repair and cell death due to DNA double strand breaks [2]. Most dUTPases are homotrimers with active sites at subunit interfaces (Fig. 2A) [3]. Oligomerization is therefore crucial to active site architecture in these enzymes.

Stability in oligomers is determined by the nature of inter-subunit interactions. Such interactions in the dUTPase homotrimer fall into three classes (Fig. 2A) [4]. First, two neighbouring subunits create apolar contacts. Second, the C-terminal β -strand of the first subunit becomes integrated into the β -stranded jelly-roll fold of the second subunit. The C-terminal arm continues in crossing over the surface of the second subunit to reach the active site that receives conserved sequence

motifs from the third subunit. Third, residues from all subunits contribute to form the central channel of the homotrimer. The three contact types were termed pairwise, arm-crossing and threefold interactions, respectively [5]. Pairwise and β -strand-swapping contacts are of highly similar character in all dUTPase homotrimers. However, threefold interactions within the central channel are greatly different. Hydrophobicity of these contacts was recently suggested to affect enzymatic mechanism in a way that linked increased polarity to cooperativity in substrate binding [6]. The major difference in threefold interactions may also significantly perturb stability of the homotrimer. In the prokaryotic enzyme, the inner channel is closely packed with apolar residues conserved among prokaryotic dUTPases. In human and *Drosophila* enzymes, only a small number of polar or charged residues are located in the channel at distances that preclude cohesive interactions except for a conserved Arg–Glu–Tyr H-bonded triad [5]. In addition to the conserved dUTPase sequence, the *Drosophila* enzyme also contains a flexible species-specific 28-residue C-terminal extension [6,7].

Here, we investigated stability of bacterial and *Drosophila* dUTPases, selected to represent pro- or eukaryotic homotrimers. Two types of denaturing forces (heat and chaotropic solvent) were applied and the unfolding process was followed by various independent experimental methods [differential scanning microcalorimetry (DSC), fluorimetry, circular dichroism (CD) and Fourier transform infrared (FT-IR) spectroscopy]. The homotrimer unfolds with no significant population of folded monomers. CD experiments demonstrate retention of some secondary structural elements after heat-induced unfolding. The bacterial enzyme, associated with packed apolar inner channel, presents considerably higher resistance against all denaturing conditions arguing that stability of the dUTPase homotrimer is mainly determined by the nature of the threefold interactions.

2. Materials and methods

Gel filtration materials were purchased from Amersham Biotech, USA, Phenol Red from Merck, Germany, dUDP from Jena Biosciences, Germany, and other chemicals from Sigma, US. α,β -Imino-dUTP was synthesized as in [6]. Enzymes were expressed and purified as previously [7,8]. Protein concentration was measured spectrophotometrically using $A_{1\text{cm}}^{0.1\%_{280\text{nm}}} = 0.32, 0.26, \text{ or } 0.52$, for the *Drosophila* dUTPase constructs 1–159 (termed truncated), 1–187 (termed full-length), or bacterial dUTPase, respectively, [9]. Enzymatic activity was assayed by the continuous spectrophotometric method in 1 mM TES/HCl, pH 7.5, containing 40 μM dUTP, 5 mM MgCl_2 , 150 mM KCl, and 40 μM Phenol Red (assay buffer) ([7,10]).

* Corresponding author.

E-mail address: vertessy@enzim.hu (B.G. Vértessy).

Abbreviations: α,β -Imino-dUTP, 2'-deoxyuridine 5'-(α,β -imino)triphosphate; dUTPase, dUTP pyrophosphatase; DSC, differential scanning calorimetry; CD, circular dichroism; FT-IR, Fourier transformed infrared spectroscopy; GuHCl, guanidine hydrochloride

92 2.1. CD measurements

93 Far UV CD spectra were recorded on a JASCO 720 spectropolarimeter in 1 mm pathlength thermostatted cuvette at 25 °C, using protein samples at 0.2 mg/ml concentration in 20 mM Hepes buffer, pH 7.5, containing 5 mM MgCl₂ and 1 mM DTT (standard buffer). 96 For denaturant-induced unfolding, guanidine hydrochloride (GuHCl) or urea was added to final concentrations from 0 to 8 M. For denaturation at high pH, the standard buffer was titrated by NaOH to reach pH 14. Heat-induced unfolding measurements were carried out in standard buffer also containing 10 mM KCl. Spectra were recorded at every second degree in the temperature range 20–80 °C. After reaching 80 °C, samples were cooled back to 20 °C.

104 2.2. FT-IR measurements

105 Infrared spectra were recorded on a Bruker IFS-28 FT-IR spectrometer, equipped with a DTGS detector. *Escherichia coli* dUTPase in 25 mM sodium phosphate buffer, pH 7.5, was lyophilized. Prior to the infrared experiments, the sample was dissolved in D₂O to a final concentration of 6 mg/ml and then measured between a pair of CaF₂ windows with 110 μm pathlength. Sample temperature was controlled by a thermostatted cell jacket. Spectra were obtained at 25, 35, 50, 60 and 70 °C (this latest value was the maximum allowed for the instrument). For each temperature, 128 scans were averaged. To decrease the water vapour lines, wet-air spectra were subtracted from the protein solution spectra in the wavenumber region of 1600–1700 cm⁻¹. The corrected spectra were deconvoluted using the built-in software of the Origin 5.0 package relying on Lorentzian curve fitting. During fitting, initial peak positions were based on second derivative spectra.

119 2.3. Analytical gel filtration

120 Protein samples in standard buffer also containing 3 M GuHCl were applied on Superdex 200HR column in a total volume of 100 μl, at a concentration of 5–10 mg/ml, with a flow rate of 0.5 ml/min. Alcohol dehydrogenase, ovalbumin, and lysozyme (150, 43, and 13.7 kDa, respectively) were used as molecular mass standards.

125 2.4. DSC

126 Calorimetric measurements were executed using the high sensitivity VP-DSC Microcalorimeter, following the manufacturer's instructions. Scans were recorded between 20 and 90 °C at 1 °C/min heating rate. Protein concentration was 0.2 mg/ml in 20 mM TES/HCl buffer, pH 7.5, containing 0.3 M NaCl, and 1 mM DTT. The melting temperature (*T_m*) was assigned to be the maximum of the excessive heat capacity function. Calorimetric enthalpies (ΔH_{cal}) were calculated from the area under the heat absorption curves [11]. Heat capacity functions were fitted to simple two-state transition model assuming the absence of experimentally observable intermediates. Fitted model curves were used to calculate van't Hoff enthalpies ($\Delta H_{van't Hoff}$) [11]. The effects of the nucleotide substrate ligands, tested at several different concentrations, were shown to level off at 5 mM dUMP, 250 μM dUDP or 100 μM dUPNPP, respectively. These ligand concentrations were therefore assumed to be saturating and Mg²⁺ was used at 5 mM concentration in the experiments.

142 2.5. Fluorescence spectroscopy

143 Samples of bacterial dUTPase in standard buffer at 0.2 mg/ml concentration were measured using a JOBIN Fluoromax-3 spectrofluorimeter, in 1 ml thermostatted cuvettes. Tryptophyl emission spectra were recorded between 295 and 390 nm with excitation at 275–280 nm. For denaturant-induced unfolding, protein samples were incubated at varied denaturant concentrations ranging 0–6 M for 1 h on ice, and spectra were recorded at 25 °C. Reversibility of GuHCl-induced unfolding was checked by enzyme activity assays. Complete refolding performed by a 20-fold dilution of the protein unfolded in 4.5 M GuHCl into assay buffer at 15 °C took 40 min. Heat-induced change of fluorescence emission at 345 nm was recorded from 25 to 80 °C.

154 2.6. Data analyses

155 Raw data for heat-induced unfolding monitored by CD at 210 and 230 nm and by fluorescence emission at 345 nm were converted to the apparent fraction of native protein *F_N*, according to Eq. (1):

$$F_N = \frac{(\Theta_U + m_U T) - \Theta}{(\Theta_U + m_U T) - (\Theta_N + m_N T)} \quad (1)$$

where Θ is the observed spectroscopic signal at temperature *T*, Θ_N and Θ_U are the intercepts and m_N and m_U the slopes of the pre- and post-translational base lines of the raw data, respectively. The *F_N*-*T* plot was then fitted to a two-state model using Eq. (2):

$$F_N = \frac{1}{1 + e^{[\Delta H(T/T_m - 1) + \Delta C_p(T_m - T - T \ln(T/T_m))]/RT}} \quad (2)$$

Initial estimates of *T_m*, ΔH_{cal} and the excessive heat capacity (ΔC_p) were from DSC experiments. The *F_N*-*T* plot was converted into the *F_U*-*T* plot by using the *F_N* + *F_U* = 1 equation, where *F_U* is the fraction of unfolded protein. Data from the excessive heat capacity function (DSC scans) were transformed into *F_U*-*T* plots by integration.

Raw data of GuHCl-induced equilibrium unfolding were fit to a two-state model using Eq. (3):

$$\Theta = \frac{\Theta_N + \Theta_U \left\{ \exp \frac{m[D] - m[D]_{50\%}}{RT} \right\}}{1 + \left\{ \exp \frac{m[D] - m[D]_{50\%}}{RT} \right\}} \quad (3)$$

where Θ is the observed spectroscopic signal measured at the actual concentration of the denaturant [D], Θ_N and Θ_U are the signals of the native and unfolded states, respectively, $[D]_{50\%}$ is the denaturant concentration at which the protein is 50% unfolded, *m* is the dependence of free energy on denaturant concentration (high *m* values indicating highly cooperative transitions), and *T* is the temperature at which the experiment was performed (25 °C).

3. Results and discussion

3.1. Two-state unfolding of dUTPases

Drosophila dUTPases 1–187 (full-length) and 1–159 (truncated, lacking the 28-residue fly-specific C-terminal extension) show *T_m* around 53 °C, while bacterial dUTPase melts at 74.5 °C (cf. [7], Fig. 1A). The significantly larger calorimetric enthalpy of the truncated 1–159 *Drosophila* dUTPase indicates that the 28-residue C-terminal extension may induce some destabilization of the folded protein, probably due to its high level of intrinsic disorder. To decide if binding of nucleotides or the Mg²⁺ co-factor induces any stabilizing effects on the protein, DSC scans were recorded in the presence of ligands. In previous experiments, saturating ligand concentrations were estimated from room-temperature dissociation constants [7]. In the present work, however, ligand saturation was tested experimentally anticipating heat-induced destabilization of protein–nucleotide complexes. In addition, the effect of the α,β -imino-dUTP, not probed previously, was also assessed.

Neither ligand induces any increment in *T_m* of bacterial dUTPase (Table 1). Nevertheless, binding of dUDP and, especially, that of α,β -imino-dUTP significantly increases ΔH_{cal} (Fig. 1B). In contrast, Mg²⁺-binding to *Drosophila* dUTPases leads to a minor, but significant *T_m* increment, with gradual further increments in the presence of dUMP and α,β -imino-dUTP (Fig. 1C, Table 1). It is worthwhile to note that even the most stable *Drosophila* enzyme complex shows a much lower *T_m* than the bacterial protein. The dUDP inhibitor, previously shown to result in a dead-end enzyme complex [7,12], has smaller stabilizing effect on the fruitfly enzyme as compared to dUMP. This observation is in contrast with the previous finding where dUMP caused smaller effect [7]. The discrepancy is quite probably due to the increased concentration of the dUMP ligand in the present work, required for saturation during the melting process. The present data show that under saturating ligand concentrations, binding of the dUDP β -phosphate to dUTPase does not induce any further stabiliza-

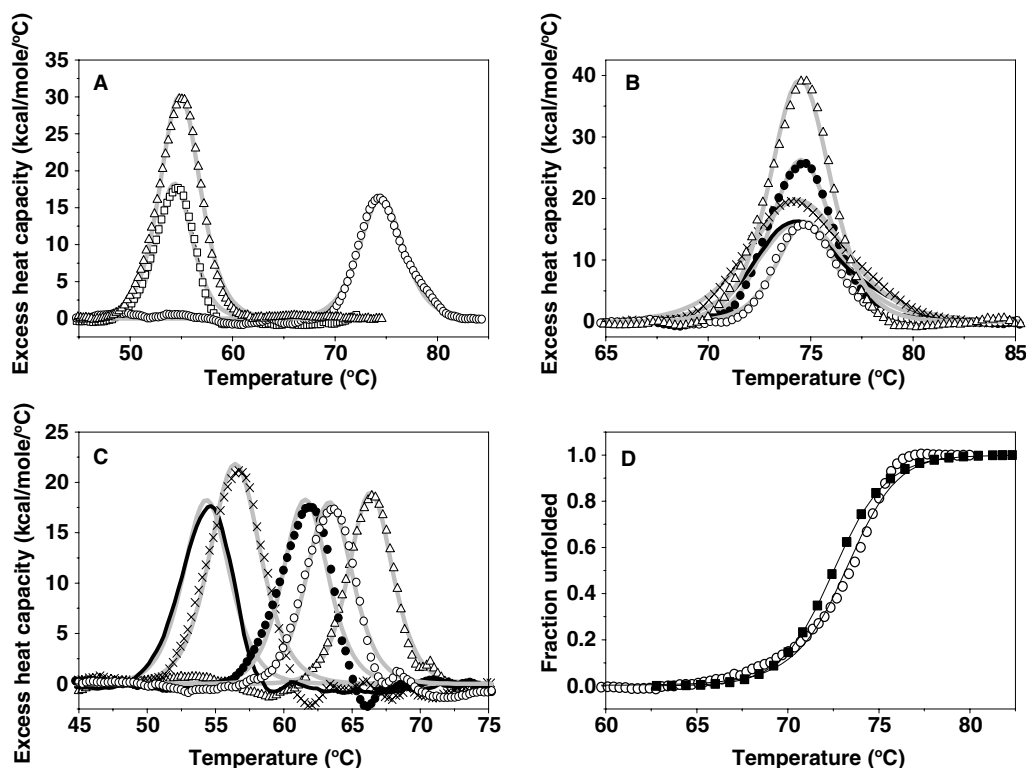


Fig. 1. Heat-induced unfolding of *Drosophila* and bacterial dUTPases. (A) Denaturation thermograms of *Drosophila* (1–159) dUTPase (Δ), *Drosophila* (1–187) dUTPase (\square) and bacterial dUTPase (\circ), characterized with $\Delta H_{\text{cal}}/\Delta H_{\text{van't Hoff}}$ ratios of 0.97, 0.44, and 0.55, respectively. (B) and (C) Heat-induced denaturation of bacterial and *Drosophila* (1–187) dUTPase, respectively, without any ligand (solid line), in the presence of 5 mM MgCl_2 (crosses), with Mg^{2+} and 5 mM dUMP (\circ), with Mg^{2+} and 250 μM dUDP (\bullet), and with Mg^{2+} and 100 μM dUPNPP (Δ). $\Delta H_{\text{cal}}/\Delta H_{\text{van't Hoff}}$ ratios range from 0.40 to 0.90. (D) Comparison of thermal denaturation of bacterial dUTPase followed by partial heat capacity (\blacksquare), as well as tryptophan fluorescence (\circ), this latter measured at 280 nm excitation wavelength. Details of F_U-T plots are described in Experimental section. ΔH_{cal} , ΔC_p and T_m parameters for best fits were 92.8 kcal/mol, 0.85 kcal/mol/°C, 72.5 °C, and 92.8 kcal/mol, 0.85 kcal/mol/°C, and 73.1 °C, for the partial heat capacity and fluorimetric data, respectively.

Table 1
Melting temperatures of dUTPases, as determined in DSC experiments

Ligand added	<i>E. coli</i> dUTPase	Truncated <i>D. melanogaster</i> dUTPase	Full-length <i>D. melanogaster</i> dUTPase
None	74.5	54.9	54.4
Mg^{2+}	74.4	55.9	56.5
Mg^{2+} + dUMP	74.8	63.1	63.4
Mg^{2+} + dUDP	74.6	62.1	61.6
Mg^{2+} + α,β -imino-dUTP	74.5	64.6	66.4

Temperatures are given in °C.

216 tion of the enzyme, in agreement with previous limited tryptophan
217 fluorescence results [7].

218 To account for the ligand-induced conformational changes
219 underlying the observed T_m increments, the ordering of the C-
220 terminal conserved Motif 5, present in all dUTPases, should be
221 considered. This ordering occurs in the same way in *Drosophila*
222 dUTPase upon binding of either dUMP, dUDP or α,β -imino-
223 dUTP [6], while it is induced only in the α,β -imino-dUTP-
224 enzyme complex of bacterial dUTPase [13,14]. Therefore, the
225 altered effects with the three nucleotides in the *Drosophila*
226 system, and no T_m increasing effect in the bacterial system by
227 any nucleotide cannot be fully explained by the C-terminal
228 conformational shift on its own but suggest some additional
229 structural change. Previous results in *Drosophila* enzyme-li-
230 gand complexes have, in fact, demonstrated that nucleotide

binding results in increased resistance against proteolysis at
231 multiple sites in the trimer [15].

232
233 DSC scans are indicative of protein oligomeric status dur-
234 ing thermal unfolding. The present $\Delta H_{\text{cal}}/\Delta H_{\text{van't Hoff}}$ ratios are
235 either close to unity or significantly lower (Fig. 1), arguing that
236 homotrimers melt without dissociation into monomers and
237 melting is accompanied with significant aggregation (cf. [7]).
238 Partial reversibility of thermal unfolding was ascertained by
239 multiple heating cycles, wherein heat capacity peaks were still
240 observed (data not shown). To describe homotrimer melting
241 with an independent technique, the single Trp residue of bac-
242 terial dUTPase was considered. The location of this residue
243 within the inner threefold channel of the trimer [4] renders it a
244 convenient endogenous probe to follow oligomerization status.
245 Intrinsic Trp fluorescence is highly dependent on microenvi-
246 ronment [16], with an emission red-shift and a quantum yield
247 decrease upon GuHCl-induced unfolding (cf. Fig. 5A, inset).
248 Unfortunately, this technique is not applicable to fruitfly
249 dUTPase lacking Trp residues. Fig. 1D depicts that changes in
250 the unfolded protein fraction of bacterial dUTPase during
251 heating display practically the same characteristics no matter
252 which experimental technique is used. This close agreement
253 indicates that translocation of the Trp residue of bacterial
254 dUTPase from an apolar environment within the central
255 channel to an aqueous solvent-exposed environment is con-
256 comitant with the unfolding transition associated with the

257 single heat-absorption peak of the DSC scan. Solvent-exposure
258 of Trp may occur either due to dissociation of the homotrimer
259 into folded monomers or due to complete unfolding. The first
260 alternative would necessarily require a significant heat-ab-
261 sorption peak reflecting melting of these monomers after the
262 fluorimetric transition. Lack of such peak strongly argues for
263 two-state unfolding with no folded monomers.

264 The scheme of this unfolding pathway is shown in Fig. 2B.
265 Results from fluorimetric and DSC experiments consonantly
266 demonstrate that homotrimeric dUTPases unfold in a one-step
267 transition. In this process, trimer dissociation and monomer
268 unfolding occur in a concomitant way, not separable under the
269 experimental conditions.

270 3.2. Distinct secondary structural elements with altered heat 271 stability

272 In addition to the above techniques, CD spectroscopy may
273 describe minor structural alterations, not necessarily involving
274 large enthalpy changes. Both the character and the intensity of
275 the CD spectrum of bacterial dUTPase are altered at high
276 temperature (Fig. 3A). Interestingly, the spectrum recorded at
277 high temperature develops a major shoulder in the 215–230 nm
278 wavelength range that suggests some non-native structural
279 ordering. This phenomenon is further discussed at the end of
280 the present section. In agreement with the DSC data, CD
281 spectra of heated dUTPase after recooling to room tempera-
282 ture reflected partial reversibility of thermal denaturation.

283 Interestingly, heating induced altered effects in different
284 spectral regions. Depending on the wavelength where CD is
285 measured, heating of the protein either increased or decreased
286 ellipticity, with an isosbestic point at 218 nm (Fig. 3A and B).
287 Wavelength-dependent transitions are characterized with dif-
288 ferent melting temperatures (Fig. 3C) to reflect distinct struc-
289 tural changes associated with altered enthalpies. The low
290 resolution information content of the CD spectra unfortu-
291 nately precluded direct assignment of CD transitions to dis-
292 tinct secondary structural elements. The assignment was
293 further complicated by the rather unusual CD spectrum of the

294 native dUTPase protein, which does not fully conform to the
295 spectrum characteristic for a β -structured protein (Table 2,
296 [10,17]). Based on the melting temperature values in compar-
297 ison with the DSC data, we propose that CD changes in the
298 lower wavelength regions (210 nm) may reflect local relaxation
299 of some turns close to the protein surface, increasingly exposed
300 to the solvent. These local effects do not require major en-
301 thalpy changes. The DSC heat absorption peak probably
302 corresponds to the CD transition observed in the higher
303 wavelength region (220–230 nm) reflecting the major unfolding
304 process (Fig. 3C).

305 CD spectroscopy was also adequate for investigation of
306 *Drosophila* dUTPase, where the absence of Trp residues pre-
307 vented fluorimetric measurements. CD spectra recorded during
308 thermal melting of the fruitfly enzyme (data not shown) pos-
309 sess very similar characteristics to the results obtained with
310 the bacterial enzyme; the only difference being that the 220-nm-
311 transition appears at a lower temperature in agreement with
312 the DSC scans. It seems therefore that in both eu- and pro-
313 karyotic dUTPases (i) some conformational transitions occur
314 with minor enthalpy changes, rendering them undetectable in
315 DSC measurements, and (ii) some residual structure is main-
316 tained after thermal melting.

317 This residual structure was further investigated by per-
318 forming thermal denaturation of the *E. coli* protein in the
319 presence of a variety of chemical denaturing agents. The inset
320 of Fig. 3D demonstrates that high concentration of either
321 GuHCl or urea, as well as extreme high pH (pH 14) all induce
322 significant unfolding, as reflected in perturbation of the CD
323 spectrum. In the high temperature measurements, the addi-
324 tional unfolding effect of these denaturing agents is also evi-
325 dent (Fig. 3D main panel). However, for the two chaotropic
326 agents used in these experiments, the unfolding effects are
327 much more pronounced at ambient as compared to high
328 temperature (compare CD changes induced by GuHCl at 25
329 and 80 °C, Fig. 3D inset and main panel, respectively). The
330 decreased effect of these two agents is probably due to their
331 reduced binding to the protein at high temperature [18,19]. The

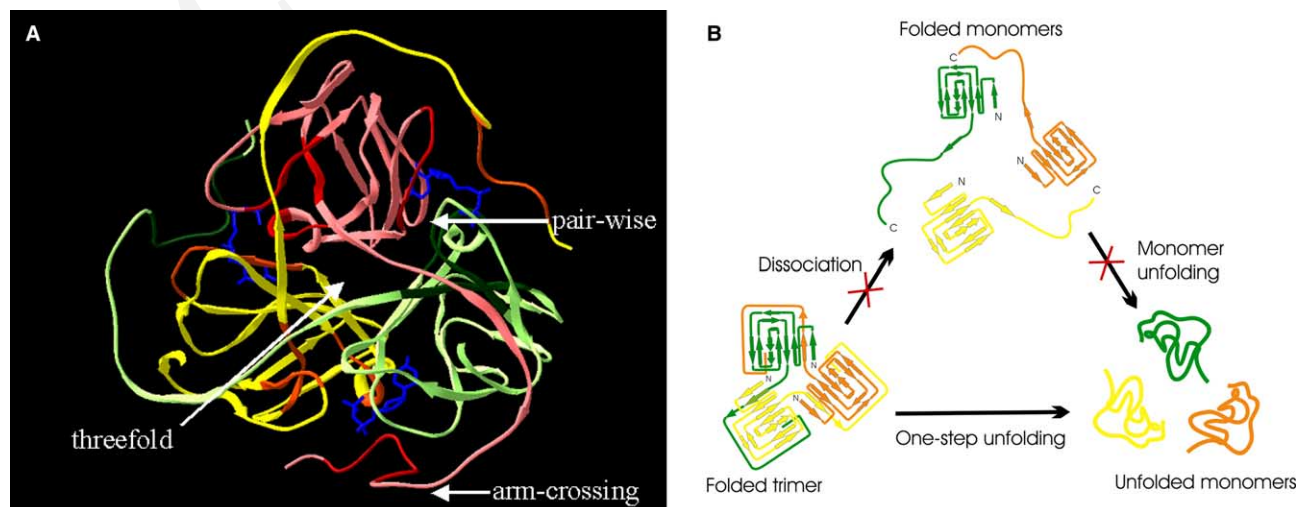


Fig. 2. Models of dUTPase structure and unfolding. (A) Monomer interactions in the dUTPase homotrimer (based on [21]). Arrows indicate the three types of interactions in ribbon representation of colour-coded oligomer, wherein the five conserved dUTPase motifs are depicted in dark shades. The dUDP ligands in the active sites are in blue colour. (B) Unfolding pathway in the dUTPase homotrimer. The model of the folded colour-coded oligomer (left) details the β -stranded jelly-roll fold.

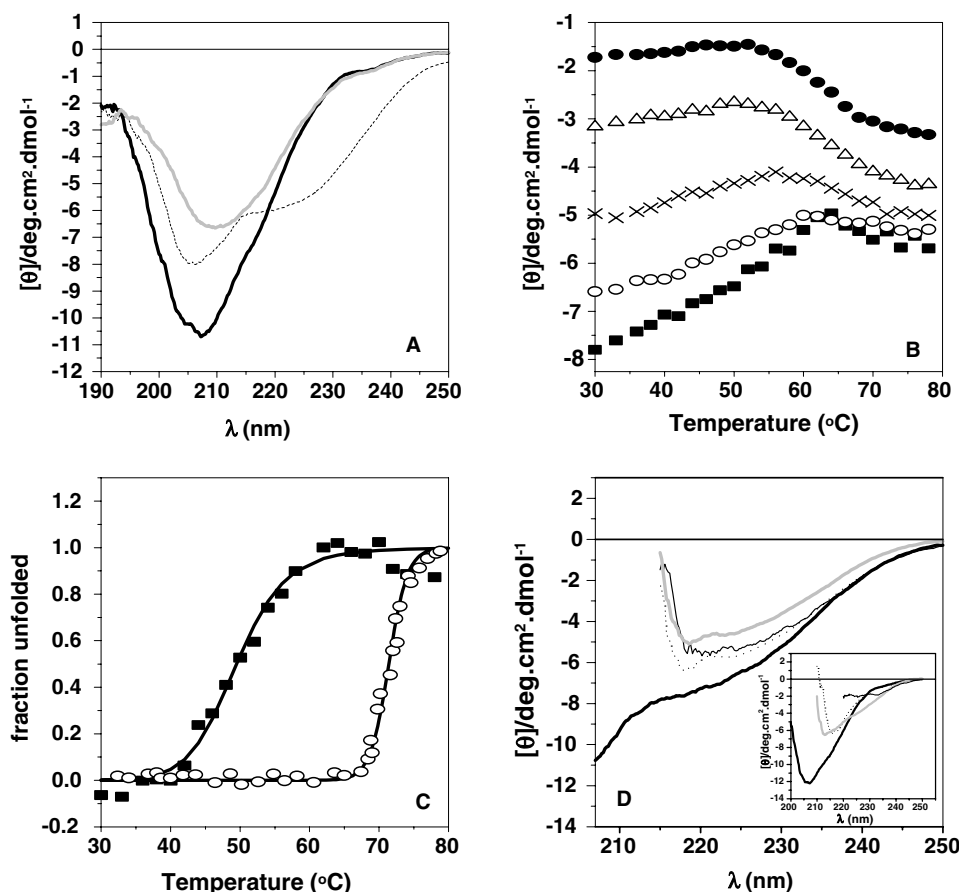


Fig. 3. Secondary structural elements during heat-induced unfolding. (A) CD spectra of bacterial dUTPase at 20 °C (solid black line), at 90 °C (dashed line), and cooled to 20 °C right after reaching 90 °C (solid grey line). (B) Temperature dependence of molar ellipticity of bacterial dUTPase at five different wavelengths, using the protein sample at 0.2 mg/ml concentration. From top to bottom: at 230 (●), 225 (△), 220 (crosses), 215 (○) and 210 (■) nm. (C) Apparent fraction of unfolded bacterial dUTPase monitored by ellipticity at 220 (○) and 210 (■) nm. The data sets were fitted to Eq. (2) (solid lines), with T_m values of 49.9 and 71.3 °C, respectively. (D, Main) CD spectra of *E. coli* dUTPase at 80 °C in the absence of denaturant (black thick line), 4.5 M GuHCl (black thin line), 8 M urea (dotted line) and at pH 14 (grey line). (D, Inset) CD spectra of *E. coli* dUTPase at 25 °C in the absence of denaturant (black thick line), 4.5 M GuHCl (black thin line), 8 M urea (dotted line) and at pH 14 (grey line).

Table 2
Estimation of secondary structural elements in *E. coli* dUTPase

Method	α -Helix (%)	β -Sheet (%)	Turn (%)	Other (%)
X-ray ^a	5	41	11	43
CD ^b	8	32	17	38
IR (35 °C)	17	48	14	21
IR (70 °C)	8	28	48	16

^a Larsson et al. [4].

^b Vertessy [10].

332 minor but significant spectral changes induced in the high
333 temperature spectrum by chemical denaturants strengthen the
334 assumption that these spectra reflect some residual secondary
335 structure that can be perturbed by chaotropes or high pH.

336 An independent spectral technique was therefore used to
337 provide more details on the protein structural elements at high
338 temperature. Fig. 4 presents FT-IR spectra of *E. coli* dUTPase
339 obtained at 35 and 70 °C in the wavenumber region character-
340 istic for amide I' band [20]. The high temperature spectrum
341 shows an increased shoulder in the 1655–1690 cm^{-1} wave-
342 number interval. Within this region, amide I' band reflects turn
343 or extended chain peptide bond conformations [20]. Based on

deconvoluted IR spectra, the relative amounts of secondary 344
structural elements were assessed (Table 2.). Although it is 345
evident that neither CD nor FT-IR can provide numerical data 346
that are in perfect agreement with those calculated based on 347
the high-resolution crystal structure, still, the temperature-in- 348
duced changes are worthwhile to examine. At high tempera- 349
ture, the decrease in both α -helical and β -sheet conformations 350
is accompanied by a significant increase in turn-like conforma- 351
tions. Results therefore suggest that high temperature may 352
induce some non-native but still ordered conformations in *E.* 353
coli dUTPase that shows FT-IR spectral characteristics remi- 354
nescent of turn-like conformations. Measurements at consid- 355
erably higher temperatures (80–90 °C), not accessible in our 356
present experimental setup, would be required for further 357
conclusive investigations of the non-native conformations in 358
the *E. coli* protein. 359

3.3. Assessing protein stability with solvent-induced denatur- 360 ation 361

Thermal unfolding studies demonstrated a major difference 362
in stability of bacterial and *Drosophila* dUTPases. This con- 363
clusion should also be tested in solvent-induced denaturation 364
experiments. As shown in the previous section, Trp fluores- 365

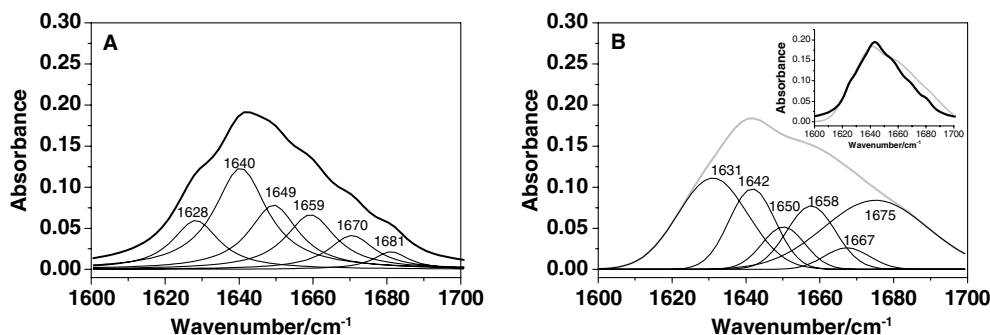


Fig. 4. FT-IR conformational analyses of *E. coli* dUTPase at 35 °C (A) and 70 °C (B). Infrared spectra of *E. coli* dUTPase at 35 °C (thick solid line) at 70 °C (thick grey line) are shown, together with the individual Lorentzian components (thin lines) obtained during deconvolution. Note the major increase of the Lorentzian at 1675 cm⁻¹ in the 70 °C-spectrum. Inset to (B) displays the measured spectra at the two different temperatures to aid direct comparison.

366 cence is a sensitive and adequate method to follow unfolding
367 of bacterial dUTPase. Fig. 5A indicates that both fluorescence
368 intensity and emission wavelength are convenient indicators to
369 follow unfolding. The process is highly cooperative, in agree-
370 ment with the data of heat-induced denaturation.

371 Unfolding of Trp-lacking *Drosophila* dUTPase cannot be
372 followed by fluorescence spectroscopy because fluorescence of
373 the *Drosophila* dUTPase Tyr residues did not show any cor-

relation to denaturant concentration, presumably due to the at
least partially solvent-exposed character of these residues even
in the folded trimer. To circumvent this problem, CD spec-
troscopy was applied. To decide if this technique generates data
comparable to those obtained by fluorescence, Fig. 5B presents
parallel measurements on bacterial dUTPase followed by both
of these methods. The D_{50%} values are in perfect agreement, but
the unfolding transition followed by CD seems to be less co-
374
375
376
377
378
379
380
381

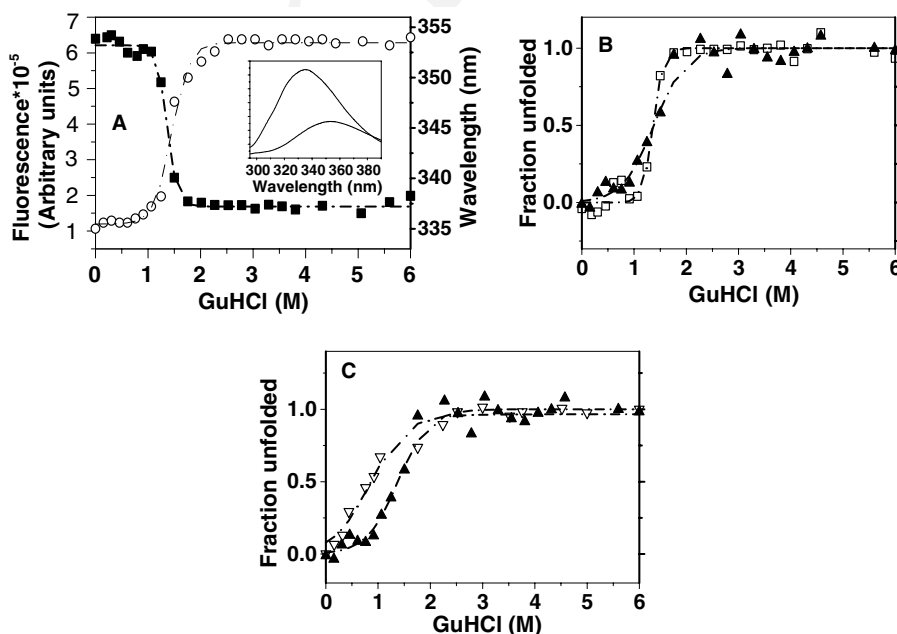


Fig. 5. GuHCl-induced unfolding of bacterial and fruitfly dUTPases. (A, Main) Tryptophan fluorescence intensity at 335 nm (■) and maximum emission wavelength (○) of bacterial dUTPase, excited at 275 nm. Raw data sets were fitted to two-state models according to Eq. (3). (A, Inset) Fluorescence spectra of native and unfolded bacterial dUTPase. From top to bottom: 0 and 6 M GuHCl. (B) Unfolded protein fraction of bacterial dUTPase from fluorescence intensity at 335 nm (□) and molar ellipticity at 222 nm (▲). (C) Unfolded protein fraction of bacterial (▲) and fruitfly dUTPase (1–159) (▽) monitored by molar ellipticity at 222 nm (▲) or 215 nm (▽).

Table 3
Denaturant *m* and D_{50%} values of dUTPases

Protein	Method	<i>m</i> (cal mol ⁻¹ M)	D _{50%} (M)
<i>E. coli</i> dUTPase	Fluorescence intensity	26 781	1.36
<i>E. coli</i> dUTPase	Fluorescence maximum emission wavelength	14 727	1.45
<i>E. coli</i> dUTPase	CD intensity	11 581	1.38
Truncated <i>D. melanogaster</i> dUTPase	CD intensity	7295	0.84

382 operative (Table 3). This difference most probably reflects that
383 several secondary structural elements are already perturbed at
384 lower denaturant concentration. However, the close agreement
385 between the $D_{50\%}$ values excludes the possibility of retention of
386 major folded structure at a state where Trp residues become
387 solvent-exposed, indicating disintegration of the trimer. This
388 result corroborates the absence of folded monomers during
389 unfolding of the oligomer (cf. Fig. 2B). Additional support is
390 provided by gel filtration data, which demonstrated trimer re-
391 tention at 3 M GuHCl (data not shown).

392 Fig. 5C shows that secondary structural elements of *Dro-*
393 *sophila* dUTPase are perturbed at the very lowest GuHCl
394 concentration indicating strikingly low stability. The signifi-
395 cant decrease in $D_{50\%}$ as compared to the value observed with
396 bacterial dUTPase provides further support to this finding.
397 Together with the thermal unfolding data, these results argue
398 for a largely increased sensitivity of fruitfly dUTPase towards
399 diverse perturbing effects.

400 3.4. Conclusions

401 Bacterial and *Drosophila* dUTPases are characterized with
402 largely different stability. The eukaryotic enzyme is signifi-
403 cantly less resistant to structural perturbations, let they be
404 induced either by heat or denaturing solvent. Similar low
405 stability was observed in the case of human dUTPase
406 (manuscript in preparation). The increased polarity of the
407 central threefold channel, which is the main structural dif-
408 ference between bacterial and eukaryotic dUTPases, is sug-
409 gested to render the latter protein more exposed to
410 environmental effects. This increased sensitivity to the envi-
411 ronment is reflected not only in decreased stability, but also
412 in ligand induced conformational changes [15], as well as in
413 cooperativity of nucleotide binding [6,7]. It seems that in-
414 creased sensitivity towards cognate ligands, presumably re-
415 quired in developed organisms, is coupled to some loss of
416 protein stability.

417 Irrespective of the overall stability, both types of dUTPases
418 were found to unfold in a process where trimer dissociation
419 and monomer unfolding cannot be separated. The scheme in
420 Fig. 2B summarizes these findings to exclude the presence of
421 natively folded monomers. This unfolding pathway underlines
422 the importance of trimeric organization in dUTPases to
423 maintain enzymatic activity.

Acknowledgements: This work was supported by grants of the Hun-
garian National Research Foundation (OTKA Grant Nos. T 034120,
TS 044730, M 27852 to B.G.V.), the Howard Hughes Medical Insti-
tutes, USA (Grant No. #55000342 to Research Scholar B.G.V.), the
Alexander von Humboldt Foundation, Germany, and the Aventis/
Institut de France Scientia Europae Prize, France (to B.G.V). We
thank István Hajdú for expert help with the FT-IR experiments.

References

- [1] Shlomai, J. and Kornberg, A. (1978) *J. Biol. Chem.* 253, 3305–33012. 432
- [2] Goulian, M., Bleile, B.M., Dickey, L.M., Grafstrom, R.H., Ingraham, H.A., Neynaber, S.A., Peterson, M.S. and Tseng, B.Y. (1986) *Adv. Exp. Med. Biol.* 195 (Pt B), 89–95. 425
- [3] Larsson, G., Svensson, L.A. and Nyman, P.O. (1996) *Nat. Struct. Biol.* 3, 532–538. 426
- [4] Gonzalez, A., Larsson, G., Persson, R. and Cedergren-Zeppezauer, E. (2001) *Acta Crystallogr. D: Biol. Crystallogr.* 57, 767–774. 427
- [5] Fiser, A. and Vertessy, B.G. (2000) *Biochem. Biophys. Res. Commun.* 279, 534–542. 428
- [6] Dubrovay, Z., Gáspári, Z., Hunyadi-Gulyás, É., Medzihradzky, F.K., Perczel, A. and Vértessy, B.G. (2004) *J Biol. Chem.* (in press). 429
- [7] Kovári, J. et al. (2004) *J. Biol. Chem.* (in press). 430
- [8] Persson, R., Nord, J., Roth, R. and Nyman, P.O. (2002) *Prep. Biochem. Biotechnol.* 32, 157–172. 431
- [9] Vertessy, B.G., Persson, R., Rosengren, A.M., Zeppezauer, M. and Nyman, P.O. (1996) *Biochem. Biophys. Res. Commun.* 219, 294–300. 432
- [10] Vertessy, B.G. (1997) *Proteins* 28, 568–579. 433
- [11] Privalov, P.L. and Potekhin, S.A. (1986) *Methods Enzymol.* 131, 4–51. 434
- [12] Larsson, G., Nyman, P.O. and Kvassman, J.O. (1996) *J. Biol. Chem.* 271, 24010–24016. 435
- [13] Vertessy, B.G., Larsson, G., Persson, T., Bergman, A.C., Persson, R. and Nyman, P.O. (1998) *FEBS Lett.* 421, 83–88. 436
- [14] Nord, J., Nyman, P., Larsson, G. and Drakenberg, T. (2001) *FEBS Lett.* 492, 228–232. 437
- [15] Kovári, J., Imre, T., Szabó, P. and Vértessy, B.G. (2004) *Nucleosides, Nucleotides Nucleic Acids* (in press). 438
- [16] Cantor, C.R. and Schimmel, P.R. (1980) *W.H. Freeman and Company, San Francisco.* 439
- [17] Greenfield, N.J. (1996) *Anal. Biochem.* 235, 1–10. 440
- [18] Poklar, N., Petrovcic, N., Oblak, M. and Vesnaver, G. (1999) *Protein Sci.* 8, 832–840. 441
- [19] Privalov, P.L. and Makhatadze, G.I. (1992) *J. Mol. Biol.* 224, 715–723. 442
- [20] Susi, H. and Byler, D.M. (1986) *Methods Enzymol.* 130, 290–311. 443
- [21] Prasad, G.S., Stura, E.A., Elder, J.H. and Stout, C.D. (2000) *Acta Crystallogr. D: Biol. Crystallogr.* 56, 1100–1109. 444

424
425
426
427
428
429
430

431

432
433
434
435
436
437
438
439
440
441
442
443
444
445
446
447
448
449
450
451
452
453
454
455
456
457
458
459
460
461
462
463
464
465
466
467
468
469
470
471
472
473